Coupling effects studied in the $^{13}C(p,pn)^{12}C$ and $^{13}C(p,d)^{12}C$ reactions at $E_p = 35$ MeV

H. Toyokawa
Research Center for Nuclear Physics, Osaka University, Osaka 567, Japan

H. Ohnuma, Y. Tajima, and T. Niizeki
Department of Physics, Tokyo Institute of Technology, Tokyo 152, Japan

Y. Honjo, S. Tomita, and K. Ohkushi
Institute of Physics, University of Tsukuba, Ibaraki 305, Japan

M. H. Tanaka and S. Kubono
Institute for Nuclear Study, University of Tokyo, Tokyo 188, Japan

M. Yosoi
Department of Physics, Kyoto University, Kyoto 606, Japan
(Received 22 November 1994)

The $^{13}C(p,pn)^{12}C$ reaction was studied at $E_p = 35$ MeV with an experimental arrangement which favored detection of p-n pairs in the $^1S_0$ state. Measured cross section angular distributions were compared with those for the $^{13}C(p,d)^{12}C$ reaction at the same incident energy. The two reactions show different angular distribution shapes, those for (p,pn) being more slowly decreasing at large angles. Coupled channel calculations which include continuum states of the p-n system reproduce angular distribution shapes and cross section magnitudes of both the (p,pn) and (p,d) data.

PACS number(s): 25.40.Hs, 24.10.Eq, 24.50.+g

I. INTRODUCTION

It is known that (d,p) and (p,d) angular distributions above incident energies of about 20 MeV cannot be described well by the distorted-wave Born approximation (DWBA) theory [1]. Experimental differential cross sections fall off more rapidly than DWBA calculations. Johnson and his collaborators proposed the adiabatic deuteron breakup approximation (ADBA) theory [2], which turned out to be very successful in explaining (d,p) and (p,d) angular distributions. According to this theory, they incoming (or outgoing) deuteron wave contains components in which it breaks up into continuum states. Such components are not described by an optical potential, nor are they included in ordinary DWBA matrix elements. The method of continuum discretized coupled channels (CDCC) [3] was developed later, which treats in a more exact manner coupling between the deuteron ground state and continuum states as well as coupling between continuum states. It has been shown from CDCC calculations that coupling with the $^3S_1$ continuum states is indeed important in (d,p) reaction amplitudes at low energies, although coupling with the D state also has noticeable effects. Coupling with the ^1P channels has been shown to improve the fit to polarization observables of deuteron elastic scattering data at several hundred MeV [4].

In addition to (d,p) and (p,d) cross sections, the CDCC theory can predict transfer cross sections from/to continuum states at the same time. However there exist no experimental data to be compared with such calculations at present. Transfer cross sections to continuum states, which can be measured in principle in (p,pn) reactions, would be very interesting since they would exhibit more direct influences of coupling effects. If outgoing p-n pairs are in the $^3S_1$ state in (p,pn) reactions, they correspond to the inverse reaction of the neutron transfer from continuum states in the (d,p) reaction, and should be strongly affected by the coupling with the bound state and between continuum states themselves. If outgoing p-n pairs are in the $^1S_0$ state, on the other hand, their center-of-mass angular distribution might be appreciably different from those for (p,d) and $(p,pn(^3S_1))$, because there is no bound $^1S_0$ state and the coupling between the $^1S_0$ and $^3S_1$ states is very weak [5]. Furthermore, the $^3D_1$ state can mix with the $^3S_1$ state through the tensor force but not with the $^1S_0$ state.

According to the analysis of low-energy p-n scattering data [6], the probability of a proton and a neutron being coupled to the $^1S_0$ state is most enhanced at zero p-n relative energy, while p-n pairs in the $^3S_1$ state show a much broader relative-energy distribution. Those in higher L states are negligible at relative energies below several MeV. Therefore, although we cannot separate p-n pairs in the $^1S_0$ state from those in the $^3S_1$ and higher L states experimentally, p-n pairs dominantly in the $^1S_0$ state could be observed if we confine our measurement to small relative-energy region. Utilizing such a technique, Cohen *et al.* have studied the (p,pn) reactions on several target nuclei with 12 and 17 MeV proton beams [7]. However, cross sections were measured only for a limited angular range in these experiments. There is also a possibility that their incident energies were low and contributions from compound processes may not have been neg-

ligible. Level densities of light nuclei are not large even around 20 MeV in excitation, and compound processes may not be averaged out to give an imaginary distorting potential for the incoming proton at these energies. In the $^{13}C + p$ channel, for instance, appreciable resonance structures are seen at least up to E_p=17 MeV [8]. In such a case the (p,d) and (p,pn) cross sections might be affected in a different way depending on the quantum numbers of a few specific compound states which incident protons happen to come across. We have measured the angular distributions of differential cross sections for the $^{13}C(p,pn)^{12}C$ and $^{13}C(p,d)^{12}C$ reactions leading to the ground state (0^+) and the 4.44 MeV state (2^+) of ^{12}C over a wide angular range and at a higher incident energy where direct reaction theories are expected to be better applicable. Enhanced detection of p-n pairs in the $^1S_0$ state was performed by measuring protons and neutrons emitted at the same angle in coincidence.

II. EXPERIMENTAL PROCEDURES AND RESULTS

The experiment was carried out using a 35-MeV proton beam from a sector focusing cyclotron at the Institute for Nuclear Study, University of Tokyo. The target was 2.0 mg/cm^2 thick self-supporting foil of enriched (99%) ^{13}C. The $^{13}C(p,d)^{12}C$ angular distributions were measured by a magnetic spectrometer [9] and a focal plane detector system [10]. In the p-n coincidence measurement, protons were detected by three pairs of Si counter telescopes, each consisting of a 0.2- or 0.4-mm-thick ΔE detector and a 2-mm-thick E detector. The solid angle of the two forward detectors was 11.6 msr, and that of the most backward detector was 13.4 msr. Neutrons were detected by three NE213 liquid scintillation counters 20.3 cm in diameter and 5.1 cm in thickness placed behind the proton detectors. Neutron energies were determined by the time-of-flight method. The flight length ranged from 162 cm to 249 cm, corresponding to the solid angle from 12.3 msr to 5.2 msr. Typical intrinsic efficiency of the neutron detector calculated by the Monte-Carlo code TOTEFF [11] was about 8% with the threshold of 2.5 MeV electron equivalent, and rather flat over the neutron energy range of interest. These efficiencies were experimentally checked by measuring the $^{13}C(p,n)^{13}N$ cross sections with the present experimental setup. The results reproduced previous data [12] within 2–4 %.

A sample two-dimensional energy spectrum of protons and neutrons in coincidence obtained at $\vartheta_p = \vartheta_n = 70°$ is shown in Fig. 1(a). Two loci corresponding to the ground state and the first excited state of ^{12}C are clearly seen. Figure 1(b) shows a sum-energy spectrum obtained from Fig. 1(a). Overall resolution of the sum-energy spectra varied from 0.8 to 1.3 MeV depending on the detection angle and the neutron flight path. A proton energy spectrum corresponding to the 4.44 MeV (2^+) state at ϑ_{lab} = 70 ° is shown in Fig. 1(c). The upper scale of this figure indicates the p-n relative energy. Enhancement due to the $^1S_0$ final state interaction is clearly seen at small relative energies. The lines are results of Monte Carlo calculations described below. Two vertical bars indicate the region used in further analysis.

We introduce the effective solid angle [13] for the $^{13}C(p,pn)^{12}C$ reaction, treating this reaction as if it were a reaction with a two-body final state, to make a direct comparison of the (p,pn) cross section with those for (p,d). In the ($\mathbf{R}$, $\mathbf{r}$) coordinate system, where $\mathbf{R} = \frac{1}{2}(\mathbf{r}_p + \mathbf{r}_n)$ and $\mathbf{r} = \mathbf{r}_p - \mathbf{r}_n$ are the center-of-mass and relative coordinates of a proton and a neutron, the triple differential cross section for the (p,pn) reaction may be factorized as

$$\frac{d^3\sigma}{d\Omega_R d\Omega_r d\varepsilon_{pn}} = C(\Omega_R)P(\varepsilon_{pn}), \quad (1)$$

where Ω_R is the effective solid angle for the center of mass of the p-n pair, Ω_r is the solid angle in the relative coordinate, and ε_{pn} is the p-n relative energy. The factor $C(\Omega_R)$ depends on the mechanism of the assumed pseudo-two-body reaction, but is independent of ε_{pn} and Ω_r except through the energy and momentum conservation. The density of states of the p-n system $P(\varepsilon_{pn})$ may

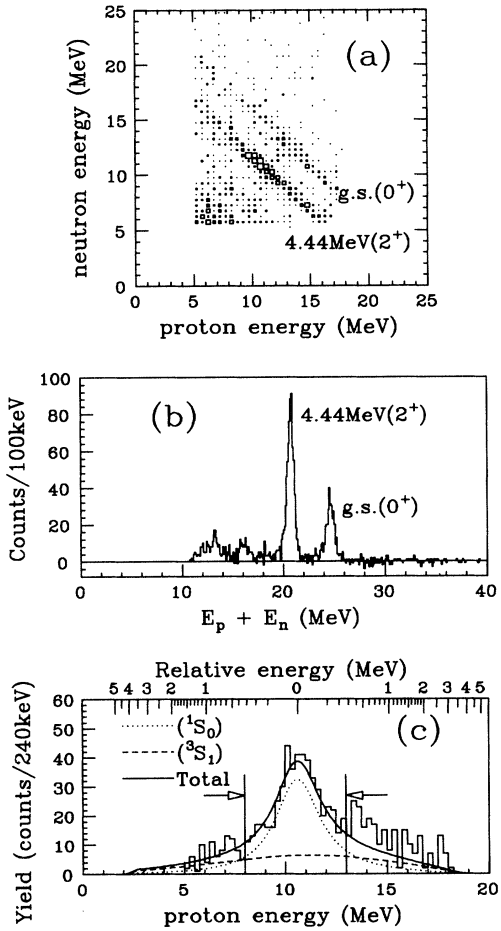

FIG. 1. (a) Two-dimensional energy spectrum and (b) sum-energy spectrum from the $^{13}C(p,pn)^{12}C$ reaction measured at E_p = 35 MeV and $\vartheta_p = \vartheta_n = 70°$. (c) Proton energy spectrum from the $^{13}C(p,pn)^{12}C$ reaction leading to the 4.44 MeV (2^+) state. Accidental coincidences have been subtracted in these spectra. The lines are Monte Carlo calculations based on the Watson-Migdal approximation. See text for details.

be given by the Watson-Migdal approximation [14] using the phase shift δ for p-n scattering. Equation (1) can be transformed to the $(\mathbf{r}_p, \mathbf{r}_n)$ coordinate system by using the Jacobian J, and the proton energy spectrum can be calculated from

$$\frac{d\sigma}{dE_p} = C(\Omega_R) \int_{\Omega_p} \int_{\Omega_n} JP(\varepsilon_{pn}) d\Omega_p d\Omega_n. \quad (2)$$

The dotted, dashed, and solid lines in Fig. 1(c) show the results for the $^1S_0$ and $^3S_1$ states and their sum, respectively, calculated from Eq. (2) using a Monte Carlo code [15]. The scattering lengths and the effective ranges used to obtain the phase shifts were taken from Ref. [6]. The energy dependence of the neutron detector efficiency and the geometrical solid angles of the proton and neutron detectors were taken into account in these calculations. The solid line is normalized to the data, but the $^1S_0$ to $^3S_1$ relative intensity, which is essentially determined by the $^1S_0$ and $^3S_1$ p-n forces, is not adjusted. The experimental points above 13 MeV are higher than the calculated curve. This is due to the inelastically scattered protons from the ^{13}C$(p,p')^{13}$C$^*(n)^{12}$C reaction passing through the ΔE-E detector. Similar fits to the data were obtained at other angles and also for the transition to the ground state. The contribution from the $^3S_1$ state is estimated from these calculations to be about 18–23 % depending on the angle, and subtracted in the following cross section calculation. However, since the $^3S_1$ contribution is rather small, we obtain an almost identical shape of the cross section angular distribution even if no subtraction is made. We will denote p-n pairs in the $^1S_0$ state thus obtained as d^* for simplicity.

Effective solid angles can be calculated from

$$\Omega_{\text{eff}} = \frac{\int_{\Omega_p} \int_{\Omega_n} \int_{E_p} JP(\varepsilon_{pn}) d\Omega_p d\Omega_n dE_p}{4\pi \int_0^{\varepsilon_{\max}} P(\varepsilon_{pn}) d\varepsilon_{pn}}, \quad (3)$$

and were 26 – 92 μsr for the $^1S_0$ state in the present experiment. The number of counts in the region indicated by two vertical bars in Fig. 1(c), after subtraction of the estimated $^3S_1$ contribution, was divided by the effective solid angle to calculate the differential cross section at each angle. They are shown in Fig. 2 together with those for (p,d). It should be noted that the effective solid angles change as well as experimental yields when we change the integration range, so that resultant differential cross sections are insensitive to the choice of the integration range. Error bars in the figures include statistical uncertainties and errors in the fitting procedure. The scale uncertainty for the (p,d) cross section is estimated to be less than 10%. That for the (p,d^*) cross section is considered to be about 20%, which include uncertainties in the subtraction of the $^3S_1$ component using the Watson-Migdal approximation and in the neutron detection efficiency. The ^{13}C$(p,d^*)^{12}$C cross sections decrease more slowly at large angles than the ^{13}C$(p,d)^{12}$C cross sections.

III. CALCULATIONS AND DISCUSSION

To compare the present data with various theories, standard DWBA and ADBA analyses for the (p,d) reaction were made first by using an exact-finite-range (EFR) DWBA code TWOFNR [16]. An optical potential given in Ref. [17] was used for the incident proton channel throughout the present analysis. The deuteron optical potential used in the EFR-DWBA calculation was taken from Ref. [18]. The real and imaginary parts of the adiabatic potentials [2] for the present ADBA analysis were calculated from

$$V(\mathbf{R}) = \frac{\int [V_p(|\mathbf{R} + \frac{1}{2}\mathbf{r}|) + V_n(|\mathbf{R} - \frac{1}{2}\mathbf{r}|)] V_{pn}(\mathbf{r}) \phi_d(\mathbf{r}) d\mathbf{r}}{\int V_{pn}(\mathbf{r}) \phi_d(\mathbf{r}) d\mathbf{r}}. \quad (4)$$

Here V_p and V_n are nucleon optical potentials obtained from Ref. [17] for the p-^{12}C and n-^{12}C systems at one half of the deuteron energy. The LS potential was taken to be the same as for the nucleon optical potential. The

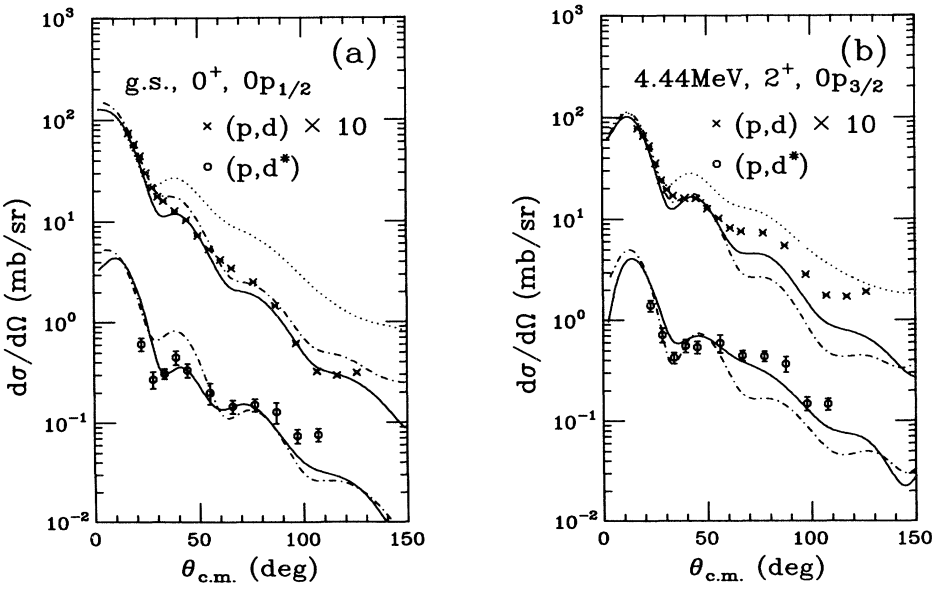

FIG. 2. Differential cross sections for the ^{13}C$(p,d)^{12}$C and ^{13}C$(p,d^*)^{12}$C reactions leading to (a) the ground state and (b) the 4.44 MeV state in ^{12}C. The dotted, dot-dashed, and solid lines are the results of DWBA, ADBA, and CDCC-CCBA calculations, respectively. See text for details.

Reid soft-core potential [19] was used for V_{pn}, and the deuteron ground-state wave function ϕ_d was its eigenfunction. The transition to the ground state of ^{12}C is a pure $0p_{1/2}$ neutron pickup, while that to the first excited state at 4.44 MeV is a pure $0p_{3/2}$ neutron pickup. The well-depth description was used to generate the form factor of the transferred neutron with parameters $r_0 = 1.25$ fm, $a = 0.65$ fm, and $V_{so} = 6.5$ MeV throughout the present calculations. The EFR-DWBA results are shown by the dotted lines, and the ADBA results by the dot-dashed lines, in Fig. 2. Calculated (p,d) cross sections were normalized to the data at forward angles to give spectroscopic factors listed in Table I together with those from the Cohen-Kurath shell model wave functions [20].

Overall shapes of the DWBA angular distributions have much slower falloff than the data. Use of different optical potential parameter sets and a folding deuteron potential [21] gives similar results. ADBA calculations better reproduce the data. These observations are consistent with a number of previous analyses [1,2], and indicate the importance of the coupling effect. It was also confirmed that the $^3D_1$ component in the deuteron ground state has a very small contribution to the (p,d) cross section at this energy. Further DWBA and ADBA calculations for the (p,d) reaction have shown that the experimentally observed differences between the (p,d) and (p,d^*) data cannot be ascribed to the 2.2-MeV difference in the Q-value or the absence of the LS term in the $^1S_0$ channel. We also tried DWBA calculations for the (p,d^*) reaction using potentials generated by folding the p-^{12}C and n-^{12}C optical potentials over the $^1S_0$ wave functions at several values of the relative wave number k_{pn}. Resultant radial shapes of the folding potential for d^* are very shallow and diffused and give structureless (p,d^*) angular distributions, in very poor agreement with the data. This may indicate that coupling between continuum states plays a key role also in the (p,d^*) reaction. Therefore ADBA calculations for the (p,d^*) reaction were tried with potentials obtained from Eq. (4) by using the $^1S_0$ wave function averaged over k_{pn}. The results shown by the dot-dashed lines in Fig. 2(b) are in fair agreement with the data, but the cross sections decrease too rapidly with the angle. Actually ADBA angular distributions for (p,d^*) are very similar to those for (p,d), and experimentally observed differences between (p,d^*) and (p,d) are not reproduced.

As an attempt to describe both the (p,d) and (p,d^*) data in a consistent manner and to include the deuteron breakup effect more explicitly, we then performed coupled-channel Born approximation (CCBA) calculations with CDCC wave functions. The codes CDC2RT and HICALST [3] were used in the CDCC calculation. The base wave functions for the bound and unbound states of the p-n system were eigenfunctions of the Reid soft-core potential V_{pn} [19]. The wave number k_{pn} for the unbound state was divided into discrete bins. The maximum values of k_{pn} were taken to be 0.81 fm^{-1} for the ground state and 0.75 fm^{-1} for the first excited state of ^{12}C. The coupling term was then calculated for each bin by using V_{pn} and p- and n-^{12}C optical potentials [17] to obtain the CDCC equations [3]. The ^3D components were mixed in the $^3S_1$ channels in the case of the (p,d) reaction, while the coupling is only between the $^1S_0$ channels in the case of the (p,d^*) reaction. Solutions of the coupled equations were then fed into TWOFNR to calculate (p,d) and (p,d^*) cross sections treating the transfer channel in the first-order Born approximation. The solid lines in Fig. 2 show the results of CDCC-CCBA calculations. They are multiplied by the spectroscopic factors given in Table I. Additional density-of-state factors are incorporated in the (p,d^*) cross sections, but no other normalizations are introduced.

The CDCC-CCBA calculations reproduce the (p,d) data very well. A considerable improvement over the ADBA calculation is observed especially for the first excited state. Although there seem to exist slight shifts to larger angles, the present CDCC-CCBA calculations also reproduce overall features of the experimental data for the (p,d^*) reaction. The angular distribution shapes for the (p,d^*) reaction as well as the (p,d^*) cross section magnitudes have been explained by the calculation. Inclusion of additional effects ignored in the present calculation, such as coupling with inelastic channels, would hopefully improve the agreement with the data.

The calculated results for the (p,d) reaction did not depend much on the maximum value of k_{pn} or on the bin size. On the other hand, it was found necessary to take as large k_{pn} values as possible for the convergence of (p,d^*) results. In other words, coupling with higher k_{pn} channels is more important in the (p,d^*) reaction. This may be due to the fact that what we are looking at in the (p,d^*) reaction are continuum states themselves while they are well defined bound deuterons in the case of the (p,d) reaction. Present analysis implies that a high-lying $^1S_0$ continuum state has more chance to come out as a p-n pair with smaller relative energy through coupling than does a high-lying $^3S_1$ state as a bound deuteron. Nevertheless, inclusion of neutron pickup to continuum states, which then come out as deuterons through the coupling,

TABLE I. Spectroscopic factors obtained from the $^{13}C(p,d)^{12}C$ and $^{13}C(p,d^*)^{12}C$ reactions.

Excitation		Transferred	Spectroscopic factor					
energy (MeV)	J^π	l_j	(p,d) [a]	(p,d) [b]	(p,d) [c]	(p,d^*) [b]	(p,d^*) [c]	Shell model [d]
0.00	0^+	$p_{1/2}$	1.0	0.7	0.8	0.8	0.8	0.61
4.44	2^+	$p_{3/2}$	1.4	1.0	1.1	1.1	1.1	1.12

[a]DWBA calculation.
[b]ADBA calculation.
[c]CDCC-CCBA calculation.
[d]Reference [20].

modifies calculated (p,d) angular distribution shapes to some extent, in agreement with a previous conclusion by Iseri [3]. Coupling between continuum states has only a minor effect on the (p,d) reaction, and major effects arise primarily from the coupling between the bound state and continuum states. On the other hand, it is the coupling between continuum states which is crucial to obtain good fits to the data in the case of the (p,d^*) reaction. The ADBA method is a reasonable approximation to include such effects, but more rigorous treatment of the coupling could appreciably improve the agreement with the data.

IV. SUMMARY

In summary, we have measured differential cross sections for the ^{13}C$(p,pn)^{12}$C and ^{13}C$(p,d)^{12}$C reactions at an incident energy of 35 MeV. The experimental setup for the (p,pn) measurement was chosen in such a way as to enhance detection of p-n pairs in the $^1S_0$ state. The two reactions show different angular distribution shapes, those for (p,pn) being more slowly decreasing at large angles. DWBA calculations cannot explain the measured (p,d) angular distributions, and inclusion of the breakup effect, either by using an adiabatic approximation or by the CDCC method, is essential to explain the (p,d) data. The CDCC-CCBA calculation is found to give not only good descriptions of the (p,d) data, but also reasonable angular distribution shapes and cross section magnitudes for the (p,pn) reaction.

The authors are indebted to Prof. M. Tanifuji, Prof. Y. Iseri, Prof. R. C. Johnson, and Prof. J. A. Tostevin for many discussions and suggestions, and to Prof. Y. Aoki and Dr. M. Masaki for their help in the CDCC calculation. One of us (H.T.) is grateful to Prof. S. M. Lee for his continuous encouragement. This work was supported in part by a Grant-in-Aid for Scientific Research, No. 01460015, from the Ministry of Education.

[1] J. L. Yntema and H. Ohnuma, Phys. Rev. Lett. **19**, 1341 (1967); H. Ohnuma, T. Suehiro, M. Sekiguchi, and S. Yamada, J. Phys. Soc. Jpn. **36**, 1236 (1974).
[2] R. C. Johnson and P. J. R. Soper, Phys. Rev. C **1**, 976 (1970); J. D. Harvey and R. C. Johnson, *ibid.* **3**, 636 (1971).
[3] Y. Iseri, M. Yahiro, and M. Nakano, Prog. Theor. Phys. **69**, 1038 (1983); M. Yahiro, Y. Iseri, H. Kameyama, M. Kamimura, and M. Kawai, Prog. Theor. Phys. Suppl. **89**, 32 (1986); M. Kawai, M. Kamimura, and K. Takesako, *ibid.* **89**, 118 (1986).
[4] J. S. Al-Khalili, J. A. Tostevin, and R. C. Johnson, Phys. Rev. C **41**, R806 (1990); Nucl. Phys. **A514**, 649 (1990); M. Tanifuji and Y. Iseri, Prog. Theor. Phys. **87**, 247 (1992).
[5] J. D. Harvey and R. C. Johnson, J. Phys. A **7**, 2017 (1974).
[6] O. Dumbrajs, R. Koch, H. Pilkuhn, G. C. Oades, H. Behrens, J. J. de Swart, and P. Kroll, Nucl. Phys. **B216**, 277 (1983).
[7] B. L. Cohen, E.C. May, and T. M. O'Keefe, Phys. Rev. Lett. **18**, 962 (1967); B. L. Cohen, E.C. May, T. M. O'Keefe, and C. L. Fink, Phys. Rev. **179**, 962 (1969); J. C. van der Weerd, T. R. Canada, C. L. Fink, and B. L. Cohen, Phys. Rev. C **3**, 66 (1971).
[8] F. Ajzengerg-Selove, Nucl. Phys. **A523**, 1 (1991).
[9] S. Kato, T. Hasegawa, and M. Tanaka, Nucl. Instrum. Methods **154**, 19 (1978).
[10] M. H. Tanaka, S. Kubono, and S. Kato, Nucl. Instrum. Methods **195**, 509 (1982).
[11] R. J. Kurz, University of California Radiation Lab. Internal Report No. UCR1-11339, 1964.
[12] H. Ohnuma, B. A. Brown, D. Dehnhard, K. Furukawa, T. Hasegawa, S. Hayakawa, N. Hoshino, K. Ieki, M. Kabasawa, K. Maeda, K. Miura, K. Muto, T. Nakagawa, K. Nisimura, H. Orihara, T. Suehiro, T. Tohei, and M. Yasue, Nucl. Phys. **A456**, 61 (1986).
[13] T. Motobayashi, S. Satoh, H. Murakami, H. Sakai, and M. Ishihara, Nucl. Instrum. Methods **A271**, 491 (1988).
[14] K. M. Watson, Phys. Rev. **88**, 1163 (1952); A. B. Migdal, Zh. Eksp. Teor. Fiz. **23**, 3 (1955) [Sov. Phys. JETP **1**, 2 (1955)].
[15] H. Okamura, computer code BREAKUP, private communication.
[16] M. Igarashi, computer code TWOFNR, private communication.
[17] B. A. Watson, P. P. Singh, and R. E. Segel, Phys. Rev. **182**, 977 (1969).
[18] G. Perrin, Nguyen Van Sen, J. Arvieux, A. Fiore, J. L. Durand, R. Darves-Blanc, J. C. Gondrand, F. Merchez, and C. Perrin, Nucl. Phys. **A193**, 215 (1972).
[19] R. V. Reid, Ann. Phys. **50**, 411 (1968).
[20] S. Cohen and D. Kurath, Nucl. Phys. **A101**, 1 (1967).
[21] S. Watanabe, Nucl. Phys. **8**, 484 (1958).